Provided for non-commercial research and education use.
Not for reproduction, distribution or commercial use.

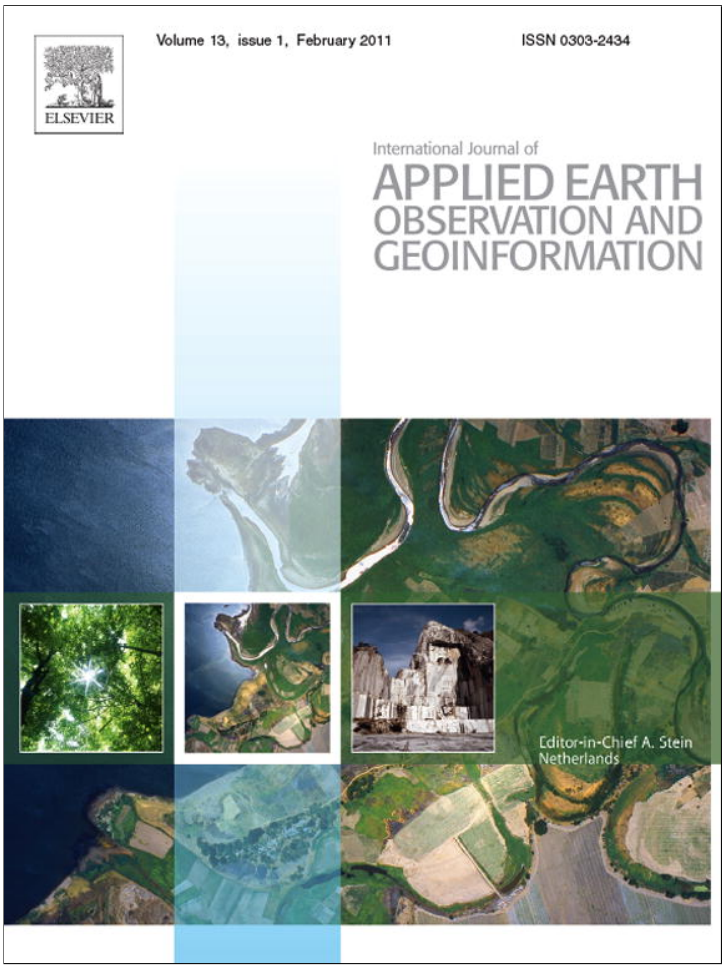

(This is a sample cover image for this issue. The actual cover is not yet available at this time.)

This article appeared in a journal published by Elsevier. The attached copy is furnished to the author for internal non-commercial research and education use, including for instruction at the authors institution and sharing with colleagues.

Other uses, including reproduction and distribution, or selling or licensing copies, or posting to personal, institutional or third party websites are prohibited.

In most cases authors are permitted to post their version of the article (e.g. in Word or Tex form) to their personal website or institutional repository. Authors requiring further information regarding Elsevier's archiving and manuscript policies are encouraged to visit:

http://www.elsevier.com/copyright

Author's personal copy

International Journal of Applied Earth Observation and Geoinformation 14 (2012) 233–244

Contents lists available at SciVerse ScienceDirect

International Journal of Applied Earth Observation and Geoinformation

journal homepage: www.elsevier.com/locate/jag

Multi-scale remote sensing sagebrush characterization with regression trees over Wyoming, USA: Laying a foundation for monitoring

Collin G. Homer[a,*], Cameron L. Aldridge[b], Debra K. Meyer[c], Spencer J. Schell[d]

[a] U.S. Geological Survey (USGS) Earth Resources Observation and Science (EROS) Center, Sioux Falls, SD, United States
[b] Department of Ecosystem Science and Sustainability and Natural Resource Ecology Laboratory, Colorado State University, in cooperation with U.S. Geological Survey, Fort Collins Science Center, Fort Collins, CO 80526, United States
[c] SGT, Contractor to the USGS EROS Center, United States[1]
[d] U.S. Geological Survey, Fort Collins, CO, United States

ARTICLE INFO

Article history:
Received 26 May 2010
Received in revised form 9 September 2011
Accepted 13 September 2011

Keywords:
Sagebrush
Wyoming
Regression tree classification
Rangeland remote sensing
Monitoring

ABSTRACT

Sagebrush ecosystems in North America have experienced extensive degradation since European settlement. Further degradation continues from exotic invasive plants, altered fire frequency, intensive grazing practices, oil and gas development, and climate change – adding urgency to the need for ecosystem-wide understanding. Remote sensing is often identified as a key information source to facilitate ecosystem-wide characterization, monitoring, and analysis; however, approaches that characterize sagebrush with sufficient and accurate local detail across large enough areas to support this paradigm are unavailable. We describe the development of a new remote sensing sagebrush characterization approach for the state of Wyoming, U.S.A. This approach integrates 2.4 m QuickBird, 30 m Landsat TM, and 56 m AWiFS imagery into the characterization of four primary continuous field components including percent bare ground, percent herbaceous cover, percent litter, and percent shrub, and four secondary components including percent sagebrush (*Artemisia* spp.), percent big sagebrush (*Artemisia tridentata*), percent Wyoming sagebrush (*Artemisia tridentata Wyomingensis*), and shrub height using a regression tree. According to an independent accuracy assessment, primary component root mean square error (RMSE) values ranged from 4.90 to 10.16 for 2.4 m QuickBird, 6.01 to 15.54 for 30 m Landsat, and 6.97 to 16.14 for 56 m AWiFS. Shrub and herbaceous components outperformed the current data standard called LANDFIRE, with a shrub RMSE value of 6.04 versus 12.64 and a herbaceous component RMSE value of 12.89 versus 14.63. This approach offers new advancements in sagebrush characterization from remote sensing and provides a foundation to quantitatively monitor these components into the future.

© 2011 Published by Elsevier B.V.

1. Introduction

Sagebrush (*Artemisia* spp.), the most common semiarid vegetation type in North America, once ranged across roughly 63 million hectare in the western United States and Canada, but today it is among the most threatened ecosystems in North America (Knick et al., 2003) and is undergoing further fragmentation and degradation (Connelly et al., 2004; Schroeder et al., 2004). The expansion of exotic plant species, altered fire frequency, intensive grazing practices, increased oil and gas development, climate change, and other factors continue to impact sagebrush ecosystems (Aldridge et al., 2008; Connelly et al., 2004; Knick et al., 2003). Coordinated ecosystem-wide analysis, integrated with monitoring and management activities, is needed to better maintain and understand the ecology and functioning of sagebrush ecosystems (Hemstrom et al., 2002), of which remote sensing could play a critical role (Booth and Tueller, 2003; Hunt Jr et al., 2003; Tueller, 1989; Washington-Allen et al., 2006).

However, semiarid shrublands such as those containing sagebrush are difficult remote sensing environments, with discrimination made difficult by sparse and similar vegetation (Graetz et al., 1988; Laliberte et al., 2007), which is often spectrally confounded by high proportions of bare ground, soil color, topography, and non-photosynthetic vegetation that all interfere with successful interpretation (Huang et al., 2010). Hence, although the need for improved remote sensing accuracy and detail in shrublands has been recognized (Tueller, 1989), much progress remains to be made (Forbis et al., 2007; Knick et al., 2003; Washington-Allen et al., 2006).

Historically, optical satellite remote sensing has been used to characterize either general land cover classes of sagebrush

* Corresponding author. Tel.: +1 605 594 2714.
E-mail address: homer@usgs.gov (C.G. Homer).
[1] Work performed under USGS contract G10PC00044.

0303-2434/$ – see front matter. © 2011 Published by Elsevier B.V.
doi:10.1016/j.jag.2011.09.012

Author's personal copy

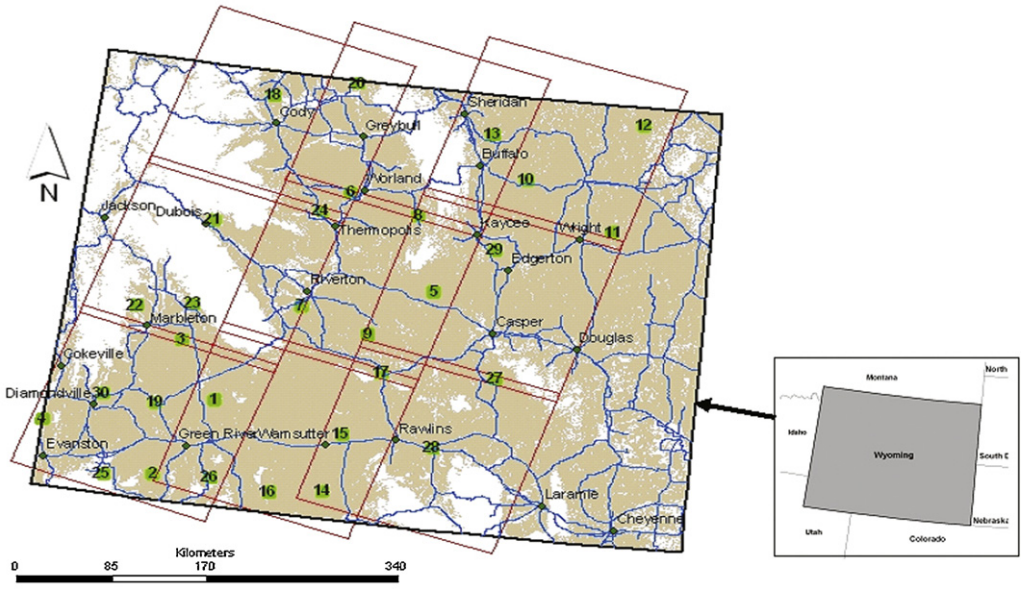

Fig. 1. Extent of landscapes targeted for development of component models for the state of Wyoming (brown). White areas represent areas excluded from analysis. Red lines indicate Landsat path/row boundaries, and green squares represent numbered QB collection sites used for training both Landsat and AWiFS imagery. AWiFS imagery covered the complete extent of the state. (For interpretation of the references to color in this figure legend, the reader is referred to the web version of the article.)

over large areas (Scott et al., 1996) or small spatial areas with more class and structural detail (Homer et al., 1993; Knick et al., 1997; Ramsey et al., 2004; Sivanpillai and Booth, 2008; Sivanpillai et al., 2009). However, for successful ecosystem-wide analysis and management, new products are needed that offer more detailed information over much larger areas and are also capable of supporting monitoring. Only one large U.S. national effort to date, the Landscape Fire and Resource Management Planning Tools Project (LANDFIRE), has attempted a more detailed sagebrush characterization over large areas (Rollins, 2009). Results may be adequate for intended National planning applications but are inadequate for other desired wildlife, range management, and climate change applications.

Optical remote sensing is the only current data source capable of cost-effectively producing ecosystem-wide products. Hence, our research seeks to further develop optical remote sensing characterization of sagebrush lands over areas large enough to provide ecosystem analysis, but with enough detail to support local adaptive resource management and change monitoring. We concluded this goal was best accomplished by the classification of a series of multiple continuous field components (four primary and four secondary components) at three spatial scales. Consequently, our research focused on deriving a method to propagate high quality field-based sampling through multiple scales of imagery in order to improve large regional component-based classifications. Steps included (1) integrating the collection of ground-measured plot data coincident with the acquisition of 2.4 m resolution imagery; (2) predicting ground-measured plot data across 2.4 m images for extrapolation on coarser imagery; (3) acquiring multiple seasons of imagery at two additional spatial scales (30 m and 56 m) for large area characterization; (4) using regression tree technology for prediction; and (5) performing rigorous accuracy assessment of component predictions.

2. Study area

Wyoming is a large, sparsely populated state in the western United States with an area of over 253,000 km^2. It contains large tracts of contiguous sagebrush lands, with an estimated 24% of all sagebrush within the U.S. Intermountain region (Connelly et al., 2004) (Fig. 1). Topographic position and exposure combined with elevation (ranging from 969 m to 4207 m) are the major determinants of plant distribution patterns (Knight, 1994).

Our research focused on elevations below 2377 m, on areas dominated by sagebrush shrubland intermingled with salt desert shrubland and grassland containing a wide variety of species. Sagebrush species include both taller and shorter growth forms, but all display a characteristic gray appearance, have relatively low chlorophyll concentrations, and typically retain their leaves year-round. Big sagebrush (*Artemisia tridentata*) is by far the most abundant sagebrush in Wyoming, other common species include black sagebrush (*A. nova*), silver sagebrush (*A. cana*), and low sagebrush (*A. arbuscula*) (Knight, 1994).

3. Materials and methods

We developed methods to integrate 2.4 m QuickBird (QB) imagery, 30 m Landsat Thematic Mapper (TM) imagery, 56 m Indian Remote Sensing Satellite Advanced Wide-Field Sensor (AWiFS) imagery, and extensive ground sampling to develop continuous field predictions with a regression tree (RT) (e.g., the percentage of the cell or pixel covered by the class viewed from overhead) for eight sagebrush ecosystem components (hereafter referred to simply as components). These include four primary components of percent bare ground, percent herbaceous cover (grass and forb), percent shrub, and percent litter and four secondary components nested within the shrub component of percent sagebrush (*Artemisia* spp.), percent big sagebrush (*A. tridentata*, representing three subspecies), percent Wyoming sagebrush (*A. tridentata wyomingensis*), and mean shrub height (centimeters). A summary of methodological approaches is presented in Table 1, with details listed below by project objective.

3.1. QB image preparation

A total of 30 QB images (64 km^2 each) were selected to support and develop regression tree predictions for nine Landsat TM path/rows and one AWiFS path/row across Wyoming (Fig. 1). QB images were specifically selected to span a reasonable range of

Author's personal copy

Table 1
Summary of multiple scale model prediction procedures for Wyoming.

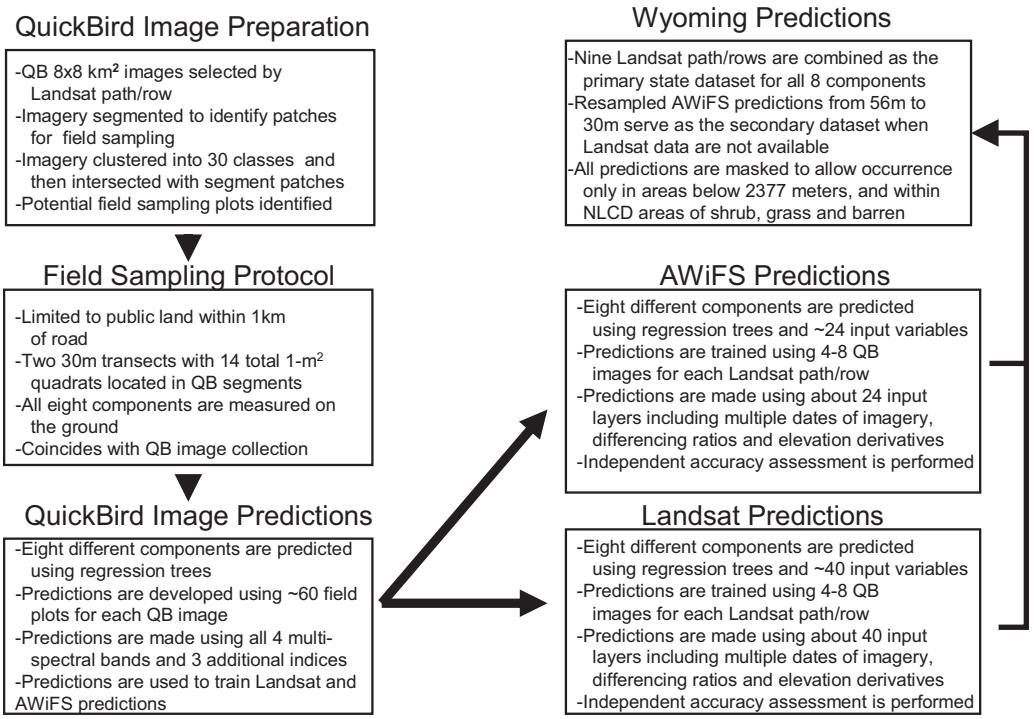

landscape diversity for each Landsat path/row. QB image location criteria included (1) representative ecological and spectral characteristics of the entire TM path/row, (2) adequate public land and road access for sampling, (3) good spatial distribution on the TM path/row, and (4) ability to represent multiple path/rows in overlap areas to facilitate edge-matching and optimize training data utilization. QB images were collected and sampled over two years, with 13 images completed in 2006 for three TM path/rows and 17 images completed in 2007 for six TM path/rows.

In order to identify homogeneous sites for potential field sampling, we used Definiens eCognition[2] software (Baatz et al., 2003) to segment the QB imagery into image objects (Homer et al., 2009). Each QB image was also per-pixel classified into 30 unsupervised clusters using an isodata algorithm in Leica Geosystems ERDAS[2] Imagine software using all four spectral bands; previous clustering trials had determined 30 clusters typically approximated the degree of spectral discrimination sufficient for our approach. Segmented polygons were then intersected with the 30 clusters to identify the majority cluster class for each polygon and essentially capture the full potential range of spectral variability across the QB image for sampling selection. Typically, two sampling polygons from each of the 30 cluster classes were selected for a minimum of ~60 sample polygons per QB image. To optimize field sampling while still capturing spectral and ecological diversity, selected polygons were further identified based on the size of the patch (>0.5 hectare), adjacency to roads (within 1 km), land ownership access, and spatial distribution on the image (no clumping). Ground sampling was completed as near to the QB acquisition date as logistically possible. If the QB image was not acquired prior to the scheduled field sampling, we applied selection procedures using 2006 1 m National Agricultural Imagery Program (NAIP) data, which were adequate for segmentation but inadequate for the modeling and prediction methods which required QB.

[2] The use of any trade, product or firm name is for descriptive purposes only and does not imply endorsement by the U.S. Government.

3.2. Field sampling protocols

Once polygons were selected within a QB image, we sampled vegetation characteristics using ocular estimation (Daubenmire, 1959; Knick et al., 1997; Mirik et al., 2007; Sant, 2005) at 14 1 m^2 quadrats along two 30 m transects within each polygon plot (Homer et al., 2009). This design facilitated quick measurement (and future re-measurement) of component abundance. For each of 14 quadrats, we estimated cover from an overhead perspective (satellite), with the total cover of all vegetation and soil components summing to 100%. Shrubs and trees were identified to the species level, except for sagebrush, which was measured at the subspecies level. All other components within the quadrat were combined into broad categories of herbaceous vegetation, litter, and bare ground. Cover measurements for shrubs were primarily based on portions of the canopy with live green vegetation. Cover measurements for herbaceous vegetation consisted of all grasses (live and residual standing) and forbs. Litter was estimated as the combined cover of dead standing woody vegetation and detached plant and animal organic matter. Bare ground included any exposed soil or rocks. All individual quadrat cover estimates were made in 5% increments. We estimated the height of each shrub or tree species by measuring the height of the tallest green vegetation (excluding seed stalks) for one representative plant within each quadrat. Because sampling teams included multiple individuals, both initial training and subsequent quality assurance oversight was instituted to maintain sampling consistency.

For application to remotely sensed data, we defined each plot as the polygon enclosed by connecting the start and end points of both transects (~0.06 ha in area, Fig. 2). We calculated a mean value for each of the eight components based on the average of all 14 1 m^2 quadrats within the plot. This mean value was then assigned to all QB pixels occurring within the plot. Within plot pixel spectral values were then evaluated, and pixels > ± one standard deviation from the mean spectral value were removed from training consideration as anomalous outliers. This resulted in a more robust training data pool and increased model prediction

Author's personal copy

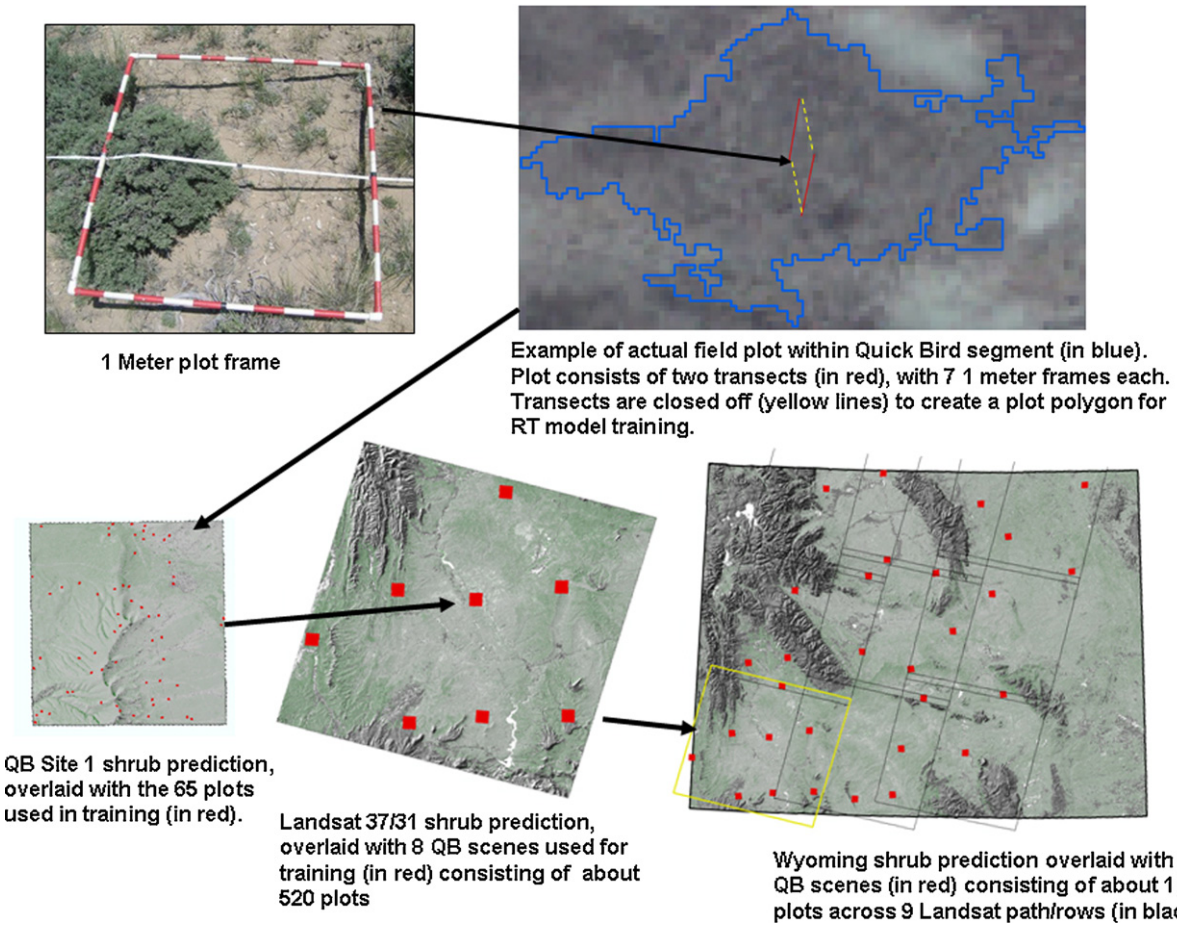

Fig. 2. Overview of field collection and training protocol for all vegetation sampling in Wyoming during 2006–2007. RT component models at all scales were ultimately extrapolated from 1 m quadrat field measurements.

accuracy at the QB level. Additionally, for some small QB heterogeneous areas our larger transects were not appropriate, and supplemental non-standardized micro-plots measured with fewer sample frames over a condensed area were used to better capture the full range of component conditions. Sample plots where spectral values were contaminated by clouds or cloud shadows were also removed from the QB model training dataset.

3.3. QB image predictions

We modeled eight components from QB images using a regression tree algorithm called Cubist[3] (Quinlan, 1993). Typically, all four 2.4 m spectral bands (Band 1 visible blue, 0.45–0.52 μm; Band 2 visible green, 0.52–0.60 μm; Band 3 visible red, 0.63–0.69 μm; and Band 4 near infrared, 0.76–0.90 μm) were used directly, with an additional three bands of ratio indices targeted for capturing Green NDVI (Band 4 – Band 2)/(Band 4 + Band 2), Moisture (Band 4 – Band 1)/(Band 4 + Band 1), and Leaf Area (Band 4)/(Band 3 + Band 2) for a total of seven spectral inputs. We developed training inputs for each component using the average component value, calculated from the aggregated quadrat measurements, within each sample plot (excluding outliers) within each QB image (typically 60 sample plots, Fig. 2). Sub-shrub secondary components were restricted to occur only in shrub areas by post-modeling masking with the shrub component. Predictions of the per-pixel percent cover for seven components as a continuous variable from 0 to 100% and shrub height (cm) were then spatially extrapolated for all pixels in each QB image.

3.4. Landsat imagery predictions

We modeled eight components using Landsat TM multi-season imagery across nine path/rows. For each component, we averaged predictions for all of the QB 2.4 m pixel values within a 30 m TM cell to create a mean rescaled value for training (Fig. 2). We then filtered 30 m cell training data by summing the four independently modeled primary components (bare ground, shrub, herbaceous, and litter) and removing cells that failed the target summation threshold of >90% or <110% judging them inadequate for training application. Thirty QB images were used to train the nine TM path/rows (Fig. 1) ranging from 4 to 8 QB images for each TM path/row.

To ensure adequate data availability across the state, in some cases we combined both 2006 and 2007 training and image information. An evaluation to compare cross-year phenology issues for path/row 37/31 indicated combining training data from both years increased RMSE error an average of 0.28 for more invariant components (shrub and sagebrush cover) and 1.3 for more variant components (bare ground and herbaceous cover). We felt this was acceptable and QB predictions from both years were combined to build training data for Landsat modeling. Further, precipitation was similar for both years, suggesting similar plant growth in both years (Wyoming State Climate Office, 2010). Approximately 40 input data layers based on multiple image dates, image band ratios, ratio

[3] The use of any trade, product or firm name is for descriptive purposes only and does not imply endorsement by the U.S. Government.

Author's personal copy

Table 2
Component prediction data input by sensor. This represents the total data made available to the regression tree for prediction.[a]

Landsat based predictions	AWiFS based predictions
Imagery, original bands	Imagery, original bands
Landsat TM, Band 1, spring, summer and fall dates	AWiFS, Band 1, spring and fall dates
Landsat TM, Band 2, spring, summer and fall dates	AWiFS, Band 2, spring and fall dates
Landsat TM, Band 3, spring, summer and fall dates	AWiFS, Band 3, spring and fall dates
Landsat TM, Band 4, spring, summer and fall dates	AWiFS, Band 4, spring and fall dates
Landsat TM, Band 5, spring, summer and fall dates	Three Ratio Index Band 1, spring and fall dates
Landsat TM, Band 7, spring, summer and fall dates	Three Ratio Index Band 2, spring and fall dates
Three Ratio Index, Band 1, spring, summer and fall dates	Three Ratio Index Band 3, spring and fall dates
Three Ratio Index, Band 2, spring, summer and fall dates	Ratio Differences Index, Band 1, spring and fall
Three Ratio Index, Band 3, spring, summer and fall dates	Ratio Differences Index, Band 2, spring and fall
Ratio Differences Index, Band 1, spring, summer and fall	Ratio Differences Index, Band 3, spring and fall
Ratio Differences Index, Band 2, spring, summer and fall	Ancillary data
Ratio Differences Index, Band 3, spring, summer and fall	Aspect, 9 Direction
Ancillary data	Elevation, Thematic classes
Aspect, 9 Direction	Slope Position Index
Elevation, Thematic classes	Slope, Degrees
Slope Position Index	
Slope, Degrees	

[a] Landsat ratios found to be most effective included Green NDVI (Band 4 – Band 2)/(Band 4 + Band 2), Moisture Index (Band 4 – Band 5)/(Band 4 + Band 5), and a Specific Leaf Area Index (Band 4)/(Band 3 + Band 7). AWiFS ratios included Green NDVI (Band 3 – Band 1)/(Band 3 + Band 1), Moisture Index (Band 3 – Band 4)/(Band 3 + Band 4), and a Specific Leaf Area Index (Band 3)/(Band 2 + Band 4). The ratio differences index for both sensors was calculated by differencing ratio derivatives between paired seasonal dates. Ancillary data were derived from the 30 m National Elevation Dataset.

differences between image dates, and 30 m ancillary topographic data derived from the National Elevation Dataset were used to build RT model predictions (Table 2). Three TM dates for each path/row were selected to represent early, middle, and late growing season conditions. All Landsat images were standardized to at-satellite reflectance before their use in the RT (Chander et al., 2009).

We created training data proportions to weight the RT to better address the full range of training data. We divided training data for each of the eight component predictions into three roughly equal bins based on the mean and original RMSE of training data values derived from cross-validation. Values less than the mean minus RMSE were grouped into a low bin, values greater than the mean plus RMSE were grouped into a high bin, and the remaining values were considered the middle bin. This approach ensured that higher and lower component predictions carried more equal weighting in model development and reduced overall bias (Wylie et al., 2008). We extrapolated predictions for all seven cover components from 0 to 100% and shrub height across all Landsat pixels by path/row (a total of 72 separate regression tree models). Sub-shrub secondary components were restricted to occur in shrub-only areas by post-modeling masking with the shrub component. Landsat individual scene results were edge-matched into a single mosaicked product by manually following land features and masked areas to create the smoothest possible transition between individual predictions. Localized remodeling of data across edge-matching boundaries was required in two small instances where the predictions were very different and required targeted models to resolve these differences.

3.5. AWiFS imagery predictions

We modeled all eight components using two seasons of AWiFS imagery across the state of Wyoming. Four separate dates in June were required to complete a 2006 June cloud-free mosaic for the state, with September requiring only one AWiFS date. No statewide cloud-free July image was available, so this date was eliminated from model development. Because of the large spatial area a single AWiFS scene covers, only a single scene from each season was required for the base image. Subsequently, we determined that the images available in standard digital number format did not need to be corrected to at-satellite reflectance. We used component predictions from the QB images and rescaled them from 2.4 m cells to 56 m cells for AWiFS to provide training data for the model predictions. All 30 QB images were used to train the AWiFS predictions. QB training data were manipulated similar to the Landsat method above. The combination of input layers used to derive model results (approximately 21 input layers for AWiFS predictions) is represented in Table 2. These input layers represent the total data made available to the RT for data mining to build model predictions for each component. Prediction, extrapolation, and accuracy assessment protocols follow the Landsat methods.

3.6. Model evaluation

Component models were evaluated in four different ways including cross-validation, independent accuracy assessment, summation testing, and LANDFIRE product comparison. Initial model evaluation was performed using a 10-fold cross-validation from the Cubist RT. Accuracy estimates were derived by using each subset to evaluate the classification developed using the remaining training samples, and their average value represents the accuracy of the classification developed using all reference samples.

An accuracy assessment was performed for the 17 QB images collected and sampled in 2007, using 12–15 extra plots collected from each image for independent evaluation of QB model predictions. Evaluation plots were selected from all sampled plots by targeting spectral categories (30 per image) that contained excess plots beyond the two required for model training. For Landsat and AWiFS accuracy assessment, we used independent plot samples collected across all TM path/rows during both years. To optimize field crew access, sample locations for component assessment were restricted to landscapes below 2377 m in elevation, on public land, within 1 km of a mapped road or trail, and within the extent of the lumped shrub, grass, and barren classes in the U.S. National Land Cover Database (NLCD 2001) (Homer et al., 2007). Independent plot selection for 2007 included initial landscape stratification using a random selection of 5 km circles, located across three site potential strata (high, medium, and low), (Wylie and Rover, 2008) that spanned potential sagebrush ecosystem situations from barren land to denser shrublands. Once initial selection was complete, a second stage random sample of eight plot locations was placed within the 5 km circle, stratified across the same site potential classes. Both 2006 and 2007 independent plot samples were combined for this assessment. Plot sampling for both years was completed using the same field protocols used for training plot collection. In order to provide an additional means of component comparison, NDVI was calculated for each sensor from the leaf-on date and regressed against independent plots to illustrate the typical photosynthetic signal available for component prediction.

Independent accuracy assessment results are reported using the coefficient of determination (R^2), the RMSE, the normalized root mean square error (NRMSE), and a linear weighted Kappa. RMSE represents an absolute measure of model fit and is in the same unit as the modeled variable (Xu et al., 2005). NRMSE is dimensionless and is calculated by dividing the RMSE by the range of

Author's personal copy

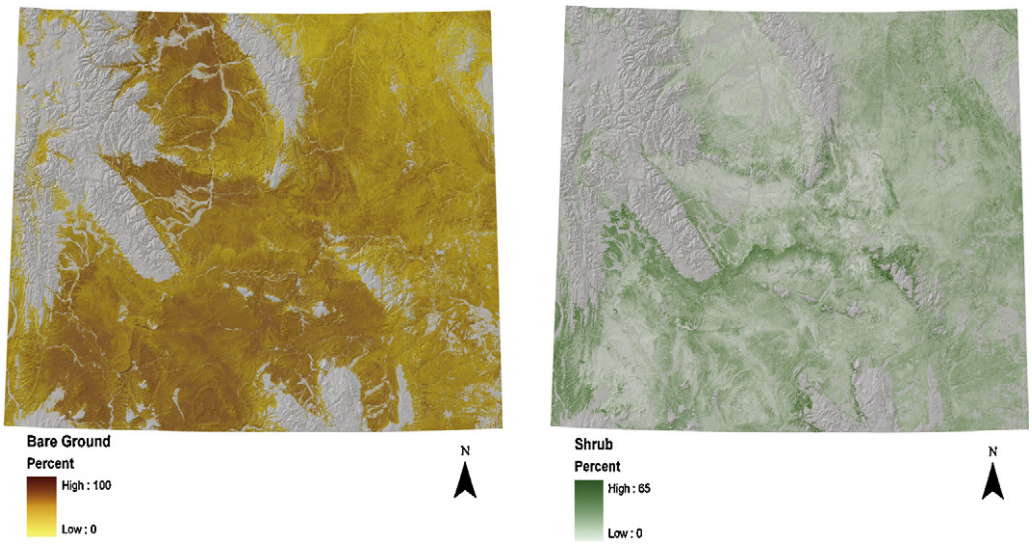

Fig. 3. Wyoming statewide predictions for bare ground and shrub from combined Landsat and AWiFS predictions. AWiFS predictions were resampled to Landsat scale (30 m) and inserted in small portions of the state not covered by the Landsat path/rows displayed in Fig. 1.

observed values to allow comparisons among different RMSE calculations and is typically expressed as a percentage. Kappa statistics were calculated for primary components using the linear weighting approach (designed for ordinal categories) to help understand error distribution within component predictions. Categories for kappa calculation were formed by grouping bare ground and herbaceous components into 10 intervals of 10% each, and litter and shrub into 10 intervals of 5% each. Litter and shrub had smaller data ranges and required 5% intervals to approximately match the number of categories created for bare ground and herbaceousness. Cross-validation and NDVI accuracy assessment results are reported using only the coefficient of determination.

An additional measure of model robustness was determined by the summation of the four primary cover components, which though created independently should ideally sum to 100% in pure rangeland areas. In order to have only pure rangeland cells evaluated, NLCD tree canopy and land cover products were used to identify and mask out potential partial rangeland pixels that contained trees or other non-rangeland content such as agriculture.

The final test of model robustness compared the results of our shrub and herbaceous component predictions to published LANDFIRE data shrub and herbaceous pixel predictions (circa 2001). The median value from the discrete 10% interval class bins for both LANDFIRE shrub and herbaceous predictions were used for comparison.

4. Results

4.1. Component predictions

A total of 2304 field plots were sampled during the summers of 2006 and 2007 across Wyoming. Of these, 1780 were used for modeling 240 component predictions across 30 QB images, 227 were withheld from model development to test subsequent QB predictions, and 297 plots were specifically sampled for model validation of the Landsat and AWiFS predictions. Using field plots, we modeled predictions for eight components for 30 2.4 m QB 64 km^2 image extents (overall 240 RT models), for 30 m Landsat across nine path/row extents (overall 72 RT models), and for 56 m AWiFS across all of Wyoming (overall 8 RT models) (Fig. 1). AWiFS predictions were used to supplement areas outside of modeled Landsat predictions to complete an entire state coverage (Fig. 3).

Component product distributions reveal bare ground with the broadest overall range and most even distribution, followed by herbaceousness and litter, which both still exhibit fairly wide ranges and distributions, especially compared to shrub (Fig. 4).

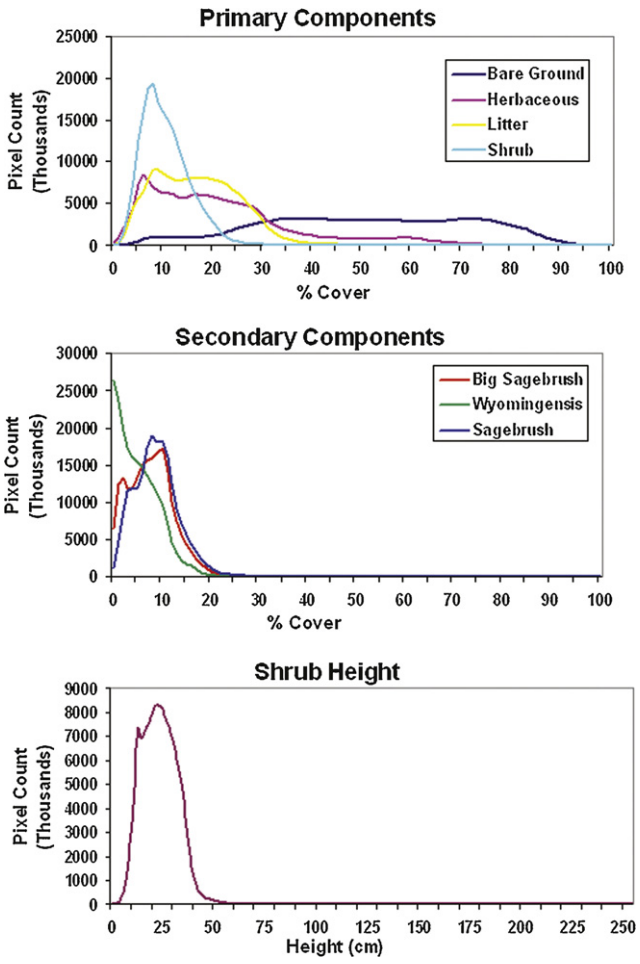

Fig. 4. Primary, secondary, and shrub height component histogram distributions for Wyoming-wide 30 m predictions.

Author's personal copy

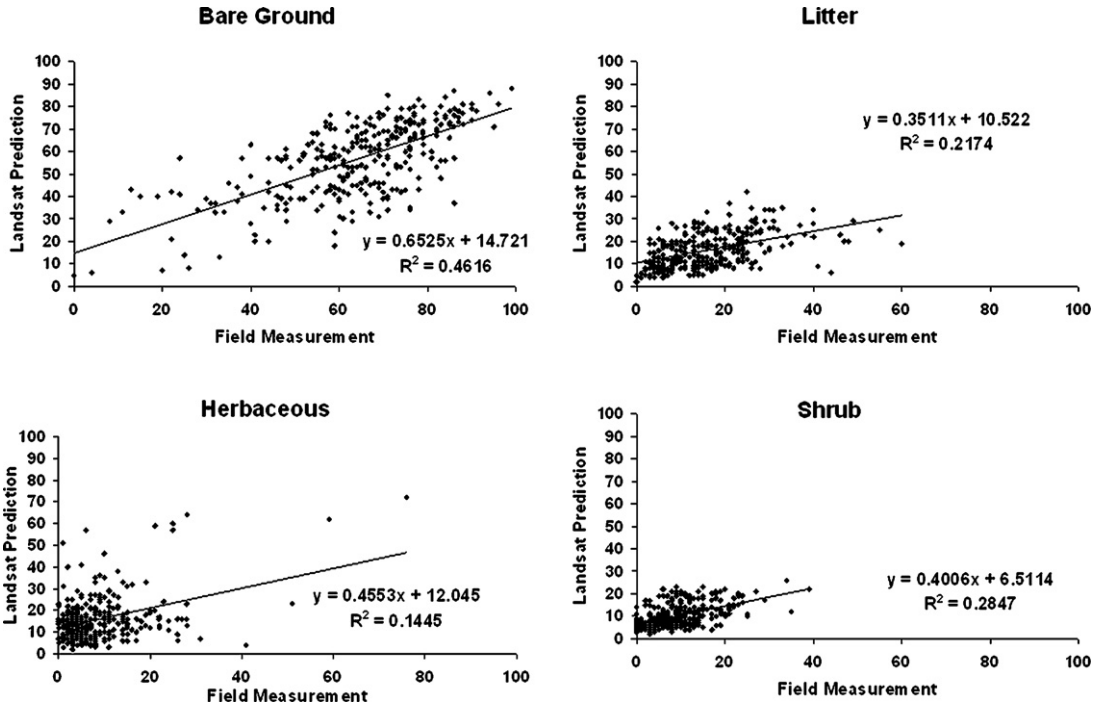

Fig. 5. Scatterplots representing the correlation between field measurements and Landsat predictions for all four primary components across Wyoming. These are based on the 297 independent field samples used for validation.

Shrub and corresponding secondary components exhibit a much more compressed range and uneven distribution, with Wyoming sagebrush having the most limited range.

4.2. Cross-validation and independent accuracy assessment

QB prediction accuracy varied by component and QB image. Overall, model cross-validation resulted in an average R^2 value across all components of 0.71, with values ranging from 0.65 for Wyoming sagebrush to 0.78 for bare ground. Independent validation results derived from the 227 field plots withheld from modeling resulted in an average R^2 value across all components of 0.51, with R^2 values ranging from 0.38 for Wyoming sagebrush to 0.71 for bare ground; all correlations were significant at $P < 0.01$. By contrast, regression of QB NDVI against field plots averaged an R^2 value of 0.18. Based on the independent evaluation, RMSE values averaged 6.52 and ranged from 4.76 for sagebrush to 10.16 for bare ground (Table 3). NRMSE values across primary component QB predictions averaged 13% (Table 3).

Landsat and AWiFS prediction accuracy varied by individual component and image path/row, and were typically more variable then QB results. Landsat model cross-validation resulted in an overall average R^2 value across all components of 0.80, with values ranging from 0.73 for shrub to 0.87 for bare ground. Independent Landsat validation results derived from 297 independently sampled field plots resulted in an average R^2 value across all components of 0.26, with R^2 values ranging from 0.14 for herbaceous to 0.46 for bare ground with all correlations significant at $P \leq 0.01$ (Fig. 5). By contrast, regression of Landsat NDVI against field plots averaged an R^2 value of 0.09. Based on the independent evaluation, RMSE values overall averaged 8.97 and ranged from 5.46 for sagebrush to 15.54 for bare ground. NRMSE values for Landsat primary predictions averaged 16, three higher than QB.

AWiFS component prediction accuracy was more variable than either Landsat or QB (Table 3). AWiFS initial model cross-validation resulted in an average R^2 value across all components of 0.65, with values ranging from 0.52 for shrub to 0.81 for bare ground. Independent AWiFS validation resulted in an average R^2 value across all components of 0.15, with R^2 values ranging from 0.08 for Wyoming sagebrush to 0.31 for bare ground with all correlations significant at $P \leq 0.01$ (Table 3). Regression of AWiFS NDVI against field plots averaged an R^2 value of 0.05. Based on the independent evaluation, RMSE values overall averaged 9.23 and ranged from 6.11 for sagebrush to 16.14 for bare ground. NRMSE values for the AWiFS primary predictions averaged 18, two higher than Landsat (Table 3).

Kappa values generated for the four primary statewide Landsat/AWiFS components after they were categorized ranged from a high of 0.38 for bare ground to a low of 0.14 for herbaceousness (Table 4). Bare ground had the widest range with values between 10 and 100%, herbaceous values had the next widest range with values between 10 and 80%, and shrub and litter values were between 5 and 40% (Fig. 6).

4.3. Summation and LANDFIRE comparison

The four primary component predictions (bare ground, herbaceousness, litter, and shrub) were summed for Landsat and AWiFS cells in range only areas. Landsat predictions had 9% of the cells summing to exactly 100%, 73% of cells summing between 95 and 105%, and 93% of cells summing between 90 and 110%. When summed for the entire state, including Landsat and AWiFS prediction areas, 8% of the cells summed to exactly 100%, 70% of the cells summed between 95 and 105%, and 92% of the cells summed between 90 and 110% (Fig. 7).

When comparing our independent accuracy assessment plots to LANDFIRE predictions, we found that our sagebrush components outperformed LANDFIRE predictions. The shrub component RMSE value was 6.04 versus 12.64 for LANDFIRE, and the herbaceous component RMSE value was 12.89 versus 14.63 for LANDFIRE (Table 5).

Author's personal copy

Table 3
Statewide model cross-validation and accuracy assessment results for seven cover components and one height component by sensor. Root mean square error (RMSE) values are in the units of model prediction (percent or height). Normalized root mean square error (NRMSE) values are expressed in percent of the total value range. NDVI results are derived from using a single date leaf-on image.

Sensor	Modeled variable	Model cross-validation	Independent validation plots				
		Mean – R^2	N	R^2	RMSE	NRMSE	NDVI R^2
QuickBird	Bare Ground (%)	0.78	229	0.71	10.16	0.11	0.47
QuickBird	Herbaceous (%)	0.74	229	0.42	6.60	0.11	0.19
QuickBird	Litter (%)	0.67	229	0.57	7.93	0.11	0.27
QuickBird	Shrub (%)	0.68	229	0.53	4.90	0.13	0.14
QuickBird	Sagebrush (%)	0.71	229	0.52	4.76	0.14	0.06
QuickBird	Big sagebrush (%)	0.70	229	0.44	4.99	0.15	0.05
QuickBird	Wyomingensis (%)	0.65	213	0.38	4.90	0.14	0.001
QuickBird	Shrub height (cm)	0.76	229	0.53	7.95	0.11	0.24
QuickBird	Mean	0.71	227	0.51	6.52	0.13	0.18
Landsat	Bare Ground (%)	0.87	297	0.46	15.54	0.16	0.23
Landsat	Herbaceous (%)	0.79	297	0.14	12.96	0.17	0.14
Landsat	Litter (%)	0.83	297	0.22	9.34	0.16	0.20
Landsat	Shrub (%)	0.76	297	0.28	6.01	0.15	0.01
Landsat	Sagebrush (%)	0.81	297	0.33	5.46	0.17	0.002
Landsat	Big sagebrush (%)	0.81	297	0.31	5.63	0.17	0.000
Landsat	Wyomingensis (%)	0.79	297	0.18	5.66	0.17	0.004
Landsat	Shrub height (cm)	0.73	297	0.15	11.20	0.17	0.09
Landsat	Mean	0.80	297	0.26	8.97	0.16	0.09
AWiFS	Bare Ground (%)	0.81	297	0.31	16.14	0.16	0.12
AWiFS	Herbaceous (%)	0.83	297	0.10	11.81	0.16	0.02
AWiFS	Litter (%)	0.66	297	0.18	9.67	0.16	0.08
AWiFS	Shrub (%)	0.62	297	0.09	6.97	0.18	0.07
AWiFS	Sagebrush (%)	0.56	297	0.15	6.11	0.19	0.05
AWiFS	Big sagebrush (%)	0.59	297	0.11	6.66	0.20	0.04
AWiFS	Wyomingensis (%)	0.64	297	0.08	6.28	0.19	0.01
AWiFS	Shrub height (cm)	0.52	297	0.18	10.18	0.16	0.04
AWiFS	Mean	0.65	297	0.15	9.23	0.18	0.05

Table 4
Kappa values for categorized interval comparison of the four primary component predictions against independent validation plots.

	Linear weighted kappa	Standard error	095 Confidence	
			Lower limit	Upper limit
Bare ground	0.383	0.031	0.315	0.438
Herbaceous	0.140	0.048	0.047	0.233
Litter	0.288	0.035	0.220	0.357
Shrub	0.307	0.035	0.240	0.375

5. Discussion

Our results demonstrate the ability of RTs to successfully parameterize all three scales of imagery into nested continuous fields for sagebrush rangelands, and further confirm the multi-spatial scaling concept previously explored (Baccini et al., 2007; Laliberte et al., 2007). However, our work took the concept one step further, producing a RT pixel-based prediction at all scales of imagery, including QB, to allow thematic nesting of all product scales. Our research advancements have centered on using optical image and ancillary input data in combination with extensive field data to develop component products that characterize a large area of sagebrush lands while still providing the capacity for local detail and quantitative monitoring.

Table 5
Shrub and herbaceous component and LANDFIRE predictions compared to independent validation plots. Cover predictions for LANDFIRE were reformatted from 10% interval categorical classes into continuous fields for this comparison.

Product	Component	N	R^2		RMSE
Sagebrush	Shrub (%)	300		0.28	6.04
LANDFIRE	Shrub (%)	300		0.07	12.64
Difference				<0.021>	<6.60>
Sagebrush	Herbaceous (%)	300		0.14	12.89
LANDFIRE	Herbaceous (%)	300		0.07	14.63
Difference				<0.07>	<1.74>

5.1. Field and QB data

We ultimately field sampled over 32,000 individual 1 m^2 quadrats across the state of Wyoming for component prediction. Given the substantial component and sensor scale differences, identifying an optimal sampling strategy is challenging (Atkinson and Curran, 1995). However, in our experience field information collected from these 1 m quadrats, and subsequently averaged over 30 m transects, remained generally effective for training the QB 2.4 m predictions. Sample site selection protocols using QB segmentation helped to optimize field collection and provide homogeneous sampling locations for QB classifications. Using QB component predictions as "super plots" for coarser scale imagery provided more abundant training data for RT model parameterization than directly using field plots could have leveraged. However, this field sampling approach was occasionally inadequate for capturing full component ranges at the QB scale, which necessitated periodic micro-plot sampling on smaller heterogeneous QB patches to measure extremes. Future transect design modifications that give additional consideration to capturing more extreme high and low component range measurements would likely improve QB RT models.

Synergizing QB image collection and field sampling (n = 30) was logistically very difficult and we achieved only varied success. Collection differences spanned a range of 1–104 days (mean difference of 39 days, with a standard deviation of 25 days). Larger differences between field sampling and image collection increased the possibility of confounding effects from phenology differences, especially with more dynamic herbaceous, litter, and bare ground components. However, there was no regional cluster pattern

Author's personal copy

Bare Ground

Prediction % Class \ Field Data % Class	10	20	30	40	50	60	70	80	90	100	total
10	2	1	1	0	0	0	0	0	0	0	4
20	0	0	1	1	2	1	0	0	0	0	5
30	1	0	1	1	2	1	2	0	0	0	8
40	0	3	2	5	8	7	5	5	1	0	36
50	0	1	2	4	4	10	19	7	1	0	48
60	0	0	1	1	6	17	16	13	6	0	60
70	0	0	0	1	1	10	21	27	4	0	64
80	0	0	0	0	0	4	12	21	24	2	63
90	0	0	0	0	0	0	0	2	4	3	9
100	0	0	0	0	0	0	0	0	0	0	0
total	3	5	8	13	23	50	75	75	40	5	297

Herbaceous

Prediction % Class \ Field Data % Class	10	20	30	40	50	60	70	80	90	100	total
10	76	12	2	1	1	0	0	0			92
20	99	33	12	0	0	0	0	0			144
30	28	9	2	0	0	1	0	0			40
40	6	5	0	0	0	0	0	0			11
50	2	0	0	0	0	0	0	0			2
60	2	0	3	0	0	0	0	0			5
70	0	0	1	0	0	1	0	0			2
80	0	0	0	0	0	0	0	1			1
90											
100											
total	213	59	20	1	1	2	0	1			297

Litter

Prediction % Class \ Field Data % Class	5	10	15	20	25	30	35	>40			total
5	7	2	4	0	0	0	0	0			13
10	13	21	13	13	3	3	0	2			68
15	8	15	14	14	11	2	0	0			64
20	3	19	14	14	15	3	2	3			73
25	2	0	7	8	10	4	2	5			38
30	1	2	8	5	4	6	2	3			31
35	0	0	0	1	1	3	2	1			8
>40	0	0	0	0	2	0	0	0			2
total	34	59	60	55	46	21	8	14			297

Shrub

Prediction % Class \ Field Data % Class	5	10	15	20	25	30	35	>40			total
5	28	10	6	1	0	0	0	0			45
10	52	47	19	5	1	0	0	0			124
15	8	24	23	11	8	0	1	0			75
20	3	11	13	5	5	3	0	0			40
25	0	5	2	3	0	1	0	1			12
30	0	0	0	0	0	0	1	0			1
35	0	0	0	0	0	0	0	0			
>40	0	0	0	0	0	0	0	0			
total	91	97	63	25	14	4	2	1			297

Fig. 6. Accuracy assessment matrices for categorized interval results from comparison of the four primary component predictions against independent validation points.

observed with QB images within Landsat path/rows of either large or small sampling delays (meaning every Landsat model usually had some of each), which we assumed helped minimize some potential confounding effects. Future exploration of the component accuracy relationship caused by phenological differences between collection times is still needed.

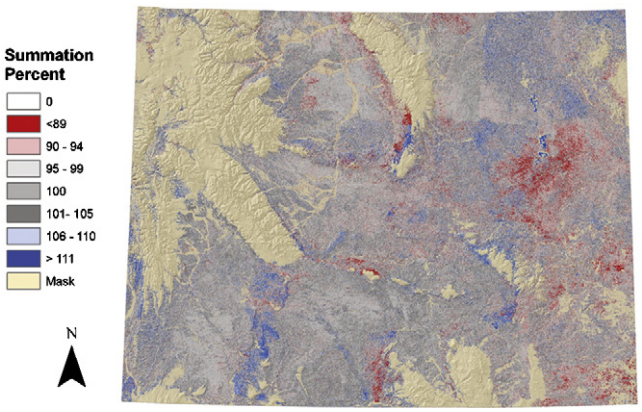

Fig. 7. The statewide summation of the four primary component predictions (bare ground, herbaceousness, litter, and shrub) for Landsat and AWiFS cells in modeled areas. Light tan areas are non-rangeland areas masked from modeling. Overall, 8% of the cells summed to exactly 100%, 70% of the cells summed between 95 and 105%, and 92% of the cells summed between 90 and 110%.

5.2. Model performance

Representing and understanding overall model performance over such a large area with so many independent models (72 at the Landsat level alone) is a complex undertaking. Only validation results averaged across many models are presented here, with further analysis of localized results beyond the scope of this paper. However, we report model performance using different statistical measures and data comparison scenarios to help present a more complete assessment and to encourage careful interpretation of product accuracy by potential users.

Overall, examination of R^2 values from correlation analysis reveals variable results by component and sensor, with Landsat having the highest mean R^2 for cross validation (possibly due to the more compressed range over QB) and QB by far the highest values from the independent assessment (Table 3). Bare ground was our best performing component prediction across all scales, which is consistent with other rangeland assessments (Booth and Tueller, 2003; Hunt Jr et al., 2003). Herbaceous component results were modest at the QB scale, but were much poorer at the Landsat and AWiFS scale. One factor in this pattern may be the more compressed ecological range of herbaceousness as the spatial scale changed over QB (see Fig. 5 scatterplot). Poor results are also likely the result of confounding phenological error introduced through the QB prediction training or the impact of combining across year (2006 and 2007) Landsat data for component generation. Secondary shrub components of sagebrush and big sagebrush also had relatively low R^2 values at the Landsat and AWiFS level, with Wyoming

Author's personal copy

sagebrush and shrub height exhibiting especially poor R^2 values. However, our big sagebrush results were similar to those reported by Jakubauskas et al. (2001), who used a RT with multitemporal SPOT reflectance data in a Wyoming sagebrush environment in Grand Teton National Park. However, they report higher R^2 results for bare ground (0.66) and shrub height (~0.46), which is likely a function of both higher spatial resolution imagery and more localized models compared to our large-area estimates. Similarly, in more localized Landsat model areas classified with this method we experienced R^2 results for bare ground at 0.73 and shrub height at 0.61 (Homer et al., 2009).

The universally low R^2 values derived from comparison of image NDVI to the independent assessment plots highlight the low photosynthetic signal potentially available for classification in a sagebrush environment (Huang et al., 2010; Langs, 2004; Sivanpillai and Booth, 2008). Comparison of NDVI results with component R^2 values illustrates the substantial improvement our modeling approach provides over a single model using NDVI alone. It also suggests that discriminating shrub and sagebrush is in part dependent upon other factors than photosynthetic signal, such as canopy shadow – especially for shrub height (Colwell, 1981). The substantial difference between cross-validation R^2 values and those from the independent assessment should also be noted. Although cross-validation R^2 values are typically optimistic, the larger than expected difference suggests some of our RT models were still not robust enough for the complexity of all unseen pixels, and model parameterization could still be improved.

RMSE is potentially the single most useful metric for gauging our product utility. Mean RMSE across all canopy components (excluding shrub height) averaged 6.32 for QB, 8.66 for Landsat, and 9.09 for AWiFS. Accuracies tended to be higher for components with greater natural ranges in their continuous fields (Fig. 4). However, the relatively small reduction in component accuracy from the QB to the Landsat and AWiFS scales is encouraging, given greater demands of extrapolating the models over a much larger spatial extent with greater ecosystem variation and complexity. RMSE values varied substantially not only by sensor but also by location. For example, across individual QB images RMSE values were both remarkably low and disappointingly high. QB site 19, which had simple topography and uniform vegetation, had RMSE values of 2.16% for sagebrush and 6.97% for bare ground, with an average RMSE across canopy components (excluding shrub height) of 3.59%. In contrast, complex topographic and vegetative QB site 30 had the greatest RMSE values of 3.76% for sagebrush and 20.58% for bare ground, with an average RMSE across all canopy components of 10.36%. Examination of the NRMSE values (Table 3) reveals that components with a much broader data range (bare ground, herbaceous, litter, and shrub height) are performing slightly better than components with compressed data ranges (shrub, sagebrush, big sagebrush, and Wyoming sagebrush; Fig. 4). NRMSE values suggest that big sagebrush is the poorest performing prediction, further highlighting the challenge of characterizing sagebrush sub-species.

In order to better understand primary component error distribution within each prediction, we categorized values to calculate an error matrix and a linear kappa. Bare ground, shrub, and litter kappa values showed fair agreement (0.38, 0.31, 0.29, respectively), with the herbaceous kappa value showing only slight agreement at 0.14 (Table 4). The order of kappa agreement is identical to the order of Landsat R^2 values for primary components (Table 3). For bare ground, the bulk of the values are distributed between 40 and 80%, with the vast majority of prediction error within 10–20% of the target class, corresponding to the 15.54 RMSE value reported for this component. Off diagonal bare ground values exhibit an under-prediction bias in the matrix. Although the herbaceous values ranged from 10 to 80%, almost all values fell in the10–30% range, creating a substantially compressed predictive data range, which likely contributed to both the lower prediction success and lower kappa value. Herbaceous values display a small over-prediction bias in the matrix. Because of their smaller overall data ranges, both shrub and litter were categorized in 5% intervals, with the majority of shrub values ranging between 5 and 20% and litter between 5 and 30%. Both components displayed off diagonal error patterns that would be expected from their RMSE values, with most shrub errors one 5% category away (RMSE 6.01) and litter error typically within two 5% categories (9.34 RMSE). Both components also displayed a slight over-predictive bias in the matrix.

5.3. Other considerations

The general pattern of loss of accuracy as grain size of imagery increases can be partly attributed to the Modifiable Areal Unit Problem (MAUP), (Jelinski and Wu, 1996) where aggregation can cause different variance patterns in the data. In our case, the modeled range of a given variable can become compressed as the spatial size of the pixel increases. Because ecological features such as shrubs have small canopies with wide spacing between individual plants, the dynamic range of cover estimates for 2.4 m pixels can range from 0 to 100%, whereas the dynamic range at 30 m cell size only varies from 0 to ~50%. Additional prediction complications also come from resistance of regression trees to adequately model outliers, further reducing the dynamic range of predicted values. While our approach of weighting training data to influence the RT to better capture the full dynamic range of the predictions helped to overcome some of the outlier issues, the influence of the MAUP and RT biases cannot be entirely overcome as scales change. Component predictions tend to be most accurate in the middle ranges, with lower accuracies at the extremes of measured values from the field.

5.4. Summation analysis and LANDFIRE comparison

Our summation analysis of the four primary components revealed 93% of all cells were within ±10% of the desired 100% target. Under-prediction areas are dominant in mountain foothills, which may contain some tree canopy cover, and in the eastern parts of the state, which has a much higher proportion of grass than shrub. Over-prediction also commonly occurs in the grass-dominated areas of eastern Wyoming, suggesting less model accuracy as grass dominance increases. Some over-prediction artifacts are also evident in some Landsat scene overlap areas, which were caused by summing unique edge-matching extents for each component. This resulted in some cells containing component predictions from two different path/rows summed into a single value (Fig. 6). However, when considering the potential individual RMSE contribution of each component, the potential for some evaluated pixels to still contain non-range elements missed in our masking, and the number of models required for our large area, 93% is a metric that seemed reasonable to us. Additionally, our shrub and herbaceous component predictions represent significant improvements over the only existing large-area product we have for comparison (LANDFIRE), which further demonstrates component improvement. However, since LANDFIRE is circa 2001 and our products are circa 2006, results should be interpreted with some caution, as some landscape change in sampled areas over this five-year interval is conceivable.

Overall, component prediction accuracy appears to have been limited most by various spatial, spectral, and ancillary data discrimination limitations which varied by sensor and location. In some models this was additionally complicated by the lack of training data robustness over unsampled areas, suggesting that even with our extensive field campaign some RT models would have further benefited from better training. Wider component range sampling

Author's personal copy

within QB areas, more careful spatial distribution of QB images on Landsat path/rows for optimizing landscape representation (Yang et al., 2003), and better matching of QB image collects and field sampling are all likely areas of future improvement. Given our extensive efforts to already involve multi-seasonal image sources in our existing RT models, future accuracy gains seem unlikely through incorporating additional image seasons; however, limiting cross-year image pooling as we were forced to do would likely reduce some error. Other new optical remote sensing sources with additional new spectral bands may also be helpful. Further accuracy improvement could likely be realized with improved ancillary source data (e.g., higher resolution Digital Elevation Models) or alternate remote sensing sources such as radar (Huang et al., 2010), hyperspectral (Mundt et al., 2006), or lidar (Sankey and Bond, 2011) that provide additional discrimination not available from traditional optical remote sensing.

Our approach of a prediction strategy with multiple spatial scales based on continuous field components is new to sagebrush characterization. We assume this approach offers a more objective way to assemble and re-measure ecosystem variables than traditional land cover mapping. Our underlying motivation for testing this multi-scale characterization approach was to design a monitoring framework that can realistically operate over large areas at a cost that is sustainable (Booth and Tueller, 2003). In our case, total potential characterization costs for the four combined primary components at our project economy of scale (in U.S. dollars) are roughly $2.00 a hectare for QB, $0.025 (2.5 cents) a hectare for Landsat, and $0.01 (one cent) a hectare for AWiFS. We assume costs for repeated measurement will be a fraction of the original characterization cost if update methods target only changing patches (Xian and Homer, 2010), keeping monitoring costs relatively low for coarser scales of imagery.

6. Conclusions

Our approach produced four primary and four secondary continuous field sagebrush components nested at three spatial scales. Methods centered on using a RT classification algorithm to make component predictions from multiple image and ancillary input layers parameterized with direct field data at the QB level, and subsequently with QB predictions as field data for Landsat and AWiFS predictions for all of Wyoming. Primary component accuracies included RMSE values ranging from 4.90 to 10.16 for 2.4 m QuickBird, 6.01 to 15.54 for 30 m Landsat, and 6.97 to 16.14 for 56 m AWiFS. Secondary component accuracies included RMSE values ranging from 4.76 to 7.95 for 2.4 m QuickBird, 5.46 to 11.20 for 30 m Landsat, and 6.11 to 10.18 for 56 m AWiFS. Landsat and AWiFS component products provide enough detail for local application, span large enough areas for ecosystem analysis, and provide a more quantitative framework for future monitoring. Research on component applications analyzing current and historical vegetation change, climate variation, sage grouse habitat distribution, and grazing trends are now in process and will be reported in subsequent papers.

Acknowledgements

We thank G. Fox, A. Krcmarik, C. Mahony, K. Moon, R. Pearce, T. Perfors, S. Rehme, J. Severson, and G. Wann, for their tireless work collecting field data, and D. Neubaum and D. Keck for their coordination of field crews. We also thank the United States Geological Survey and the United States Bureau of Land Management (BLM) who supported this project financially. Specifically, we acknowledge E.T. Rinkes, R. Vigil, K. Henke, and D. Simpson for their support and interest in this research. We also thank T. Loveland, B. Wylie, G. Xian and two anonymous reviewers for their helpful review of this manuscript.

References

Aldridge, C.L., Nielsen, S.E., Beyer, H.L., Boyce, M.S., Connelly, J.W., Knick, S.T., Schroeder, M.A., 2008. Range-wide patterns of greater sage-grouse persistence. Divers. Distrib. 14 (6), 983–994.

Atkinson, P.M., Curran, P.J., 1995. Defining an optimal size of support for remote sensing investigations. IEEE Trans. Geosci. Remote Sens. 33 (3), 768–776.

Baatz, M., Benz, U., Dehghani, S., 2003. eCognition© User Guide 3. Definiens Imaging. Munich, Germany.

Baccini, A., Friedl, M.A., Woodcock, C.E., Zhu, Z., 2007. Scaling field data to calibrate and validate moderate spatial resolution remote sensing models. Photogramm. Eng. Remote Sens. 73 (8), 945–954.

Booth, D.T., Tueller, P.T., 2003. Rangeland monitoring using remote sensing. Arid Land Res. Manag. 17 (4), 455–467.

Chander, G., Huang, C., Yang, L., Homer, C., Larson, C., 2009. Developing consistent landsat data sets for large area applications: the MRLC 2001 protocol. IEEE Geosci. Remote Sens. Lett. 6 (4), 777–781.

Colwell, J.S., 1981. Landsat feature enhancement or can we separate vegetation from soil. In: Proceedings of the 15th International Symposium on Remote Sensing of the Environment, pp. 559–621.

Connelly, J.W., Knick, S.T., Schroeder, M.A., Stiver, S.J., 2004. Conservation assessment of greater sage grouse and sagebrush habitats. Western Association of Fish and Wildlife Agencies, Unpublished Report, Cheyenne, WY. Available from: http://www.ndow.org/wild/conservation/sg/resources/greate%5Fsg%5Fcons%5Fassessment.pdf (accessed November 2010).

Daubenmire, R., 1959. A canopy-coverage method of vegetational analysis. Northwest Sci. 33, 43–64.

Forbis, T.A., Provencher, L., Turner, L., Medlyn, G., Thompson, J., Jones, G., 2007. A method for landscape-scale vegetation assessment: application to Great Basin rangeland ecosystems. Rangel. Ecol. Manag. 60 (3), 209–217.

Graetz, R.D., Pech, R.P., Davis, A.W., 1988. The assessment and monitoring of sparsely vegetated rangelands using calibrated Landsat data. Int. J. Remote Sens. 9 (7), 1201–1222.

Hemstrom, M.A., Wisdom, M.J., Hann, W.J., Rowland, M.M., Wales, B.C., Gravenmier, R.A., 2002. Sagebrush-steppe vegetation dynamics and restoration potential in the interior Columbia Basin. U.S.A. Conserv. Biol. 16 (5), 1243–1255.

Homer, C., Dewitz, J., Fry, J., Coan, M., Hossain, N., Larson, C., Herold, N., McKerrow, A., VanDriel, J.N., Wickham, J., 2007. Completion of the 2001 National Land Cover Database for the conterminous United States. Photogramm. Eng. Remote Sens. 73 (4), 337–341.

Homer, C.G., Aldridge, C.L., Meyer, D.K., Coan, M.J., Bowen, Z.H., 2009. Multiscale Sagebrush Rangeland Habitat Modeling in Southwest Wyoming. U.S. Geological Survey, Open-File Report, 2009-1092.

Homer, C.G., Edwards Jr., T.C., Ramsey, R.D., Price, K.P., 1993. Use of remote sensing methods in modelling sage grouse winter habitat. J. Wildl. Manag. 57 (1), 78–84.

Huang, S., Potter, C., Crabtree, R.L., Hager, S., Gross, P., 2010. Fusing optical and radar data to estimate sagebrush, herbaceous, and bare ground cover in Yellowstone. Remote Sens. Environ. 114 (2), 251–264.

Hunt Jr., E.R., Everitt, J.H., Ritchie, J.C., Moran, M.S., Booth, D.T., Anderson, G.L., Clark, P.E., Seyfried, M.S., 2003. Applications and research using remote sensing for rangeland management. Photogramm. Eng. Remote Sens. 69 (6), 675–693.

Jakubauskas, M., Kindscher, K., Debinski, D., 2001. Spectral and biophysical relationships of montane sagebrush communities in multi-temporal SPOT XS data. Int. J. Remote Sens. 22 (9), 1767–1778.

Jelinski, D.E., Wu, J., 1996. The modifiable areal unit problem and implications for landscape ecology. Landsc. Ecol. 11 (3), 129–140.

Knick, S.T., Dobkin, D.S., Rotenberry, J.T., Schroeder, M.A., Vander Haegen, W.M., Van Riper Iii, C., 2003. Teetering on the edge or too late? Conservation and research issues for avifauna of sagebrush habitats. Condor 105 (4), 611–634.

Knick, S.T., Rotenberry, J.T., Zarriello, T.J., 1997. Supervised classification of Landsat Thematic Mapper imagery in a semi-arid rangeland by nonparametric discriminant analysis. Photogramm. Eng. Remote Sens. 63 (1), 79–86.

Knight, D.H., 1994. Mountains and Plains, the Ecology of Wyoming Landscapes. Yale University Press, New Haven, CT.

Laliberte, A.S., Fredrickson, E.L., Rango, A., 2007. Combining decision trees with hierarchical object-oriented image analysis for mapping arid rangelands. Photogramm. Eng. Remote Sens. 73 (2), 197–207.

Langs, L.A., 2004. Remote Sensing of Sagebrush Community Structural Patterns Across Scales. Utah State University, Masters Thesis.

Mirik, M., Norland, J.E., Biondini, M.E., Crabtree, R.L., Michels Jr., G.J., 2007. Relationships between remotely sensed data and biomass components in a big sagebrush (*Artemisia tridentata*) dominated area in Yellowstone National Park. Turk. J. Agric. For. 31 (2), 135–145.

Mundt, J.T., Streutker, D.R., Glenn, N.F., 2006. Mapping sagebrush distribution using fusion of hyperspectral and lidar classifications. Photogramm. Eng. Remote Sens. 72 (1), 47–54.

Quinlan, J.R., 1993. C4.5 Programs for Machine Learning. Morgan Kaufmann Publishers, San Mateo, CA.

Ramsey, R.D., Wright Jr., D.L., McGinty, C., 2004. Evaluating the use of Landsat 30 m Enhanced Thematic Mapper to monitor vegetation cover in shrub-steppe environments. Geocarto. Int. 19 (2), 39–47.

Author's personal copy

Rollins, M.G., 2009. LANDFIRE: a nationally consistent vegetation, wildland fire, and fuel assessment. Int. J. Wildland Fire 18 (3), 235–249.
Sankey, T.T., Bond, P., 2011. LiDAR-based classification of sagebrush community types. Rangel. Ecol. Manag. 64 (1), 92–98.
Sant, E.D., 2005. Identifying Temporal Trends in Treated Sagebrush Communities Using Remotely Sensed Imagery. Utah State University, Masters Thesis.
Schroeder, M.A., Aldridge, C.L., Apa, A.D., Bohne, J.R., Braun, C.E., Bunnell, S.D., Connelly, J.W., Deibert, P.A., Gardner, S.C., Hilliard, M.A., Kobriger, G.D., McAdam, S.M., McCarthy, C.W., McCarthy, J.J., Mitchell, D.L., Rickerson, E.V., Stiver, S.J., 2004. Distribution of sage-grouse in North America. Condor 106 (2), 363–376.
Scott, J.M., Tear, T.H., Davis, F. (Eds.), 1996. Gap Analysis: A Landscape Approach to Land Management Issues. American Society of Photogrammetric Engineering and Remote Sensing, Bethesda, MD.
Sivanpillai, R., Booth, D.T., 2008. Characterizing rangeland vegetation using Landsat and 1-mm VLSA data in central Wyoming (USA). Agrofor. Syst. 73 (1), 55–64.
Sivanpillai, R., Prager, S.D., Storey, T.O., 2009. Estimating sagebrush cover in semi-arid environments using Landsat Thematic Mapper data. Int. J. Appl. Earth Observ. Geoinf. 11 (2), 103–107.
Tueller, P.T., 1989. Remote sensing technology for rangeland management applications. J. Range. Manag. 42 (6), 442–453.
Washington-Allen, R.A., West, N.E., Ramsey, R.D., Efroymson, R.A., 2006. A protocol for retrospective remote sensing-based ecological monitoring of rangelands. Rangel. Ecol. Manag. 59 (1), 19–29.
Wylie, B.K., Rover, J.A., 2008. Accounting for climatic changes to reveal areas with anomalous ecosystem performance. In: USDA Forest Service Remote Sensing Applications Conference, 12th Biennial, Salt Lake City, UT, 15 April.
Wylie, B.K., Zhang, L., Bliss, N.B., Ji, L., Tieszen, L.L., Jolly, W.M., 2008. Integrating modelling and remote sensing to identify ecosystem performance anomalies in the boreal forest, Yukon River Basin, Alaska. Int. J. Digit. Earth 1, 196–220.
Wyoming State Climate Office, 2010. Wyoming Precipitation Charts and Data. Available from: http://www.wrds.uwyo.edu/sco/data/divisional_precip/divisional_precip.html (accessed November 2010).
Xian, G., Homer, C., 2010. Updating the 2001 National Land Cover Database impervious surface products to 2006 using Landsat imagery change detection methods. Remote Sens. Environ. 114 (8), 1676–1686.
Xu, M., Watanachaturaporn, P., Varshney, P.K., Arora, M.K., 2005. Decision tree regression for soft classification of remote sensing data. Remote Sens. Environ. 97 (3), 322–336.
Yang, L., Huang, C., Homer, C.G., Wylie, B.K., Coan, M.J., 2003. An approach for mapping large-area impervious surfaces: synergistic use of Landsat-7 ETM+ and high spatial resolution imagery. Can J. Remote Sens. 29 (2), 230–240.